Asian Journal of Chemistry; Vol. 36, No. 8 (2024), 1772-1780

ASIAN JOURNAL OF CHEMISTRY

https://doi.org/10.14233/ajchem.2024.31699

Influence of Fibre Loading on the Physico-Mechanical Properties of Water Hyacinth (*Eichhornia crassipes*) Fibre Reinforced Polyethylene Composites

N.A. KAUSHI ALOKA[1], R.A. JAYASINGHE[1,*], G. PRIYADARSHANA[2] and A.H.L.R. NILMINI[2]

[1]Department of Civil and Environmental Technology, Faculty of Technology, University of Sri Jayewardenepura, Homagama, Sri Lanka
[2]Department of Materials and Mechanical Technology, Faculty of Technology, University of Sri Jayewardenepura, Homagama, Sri Lanka

*Corresponding author: Tel: +94 71 4234951; E-mail: randika@sjp.ac.lk

Received: 9 April 2024; *Accepted*: 20 May 2024; *Published online*: 25 July 2024; AJC-21698

Water hyacinth (*Eichhornia crassipes*), an invasive aquatic weed, threatens ecosystems by rapidly spreading across water surfaces. However, this study investigates its potential as a fibre source for various applications. Decorticated water hyacinth fibres were mixed into a polyethylene matrix at different weight ratios (0%, 5%, 7.5%, 10% and 12.5%). The resulting composites underwent thorough physico-mechanical characterization. Tensile strength showed a non-linear relationship with fibre content with the 5% fibre composite exhibiting the highest strength at 8.6 MPa. Fractographic analysis revealed the strength reduction was due to poor interfacial bonding. Flexural and impact strength increased with higher fibre content, peaking at 10.07 MPa and 26 J m^{-1}, respectively, in the 12.5% fibre composite. Composite hardness rose from 43.9 to 45.5 Shore D with fibre inclusion, while density decreased. Moisture absorption and flammability increased with fibre content. This study highlights the potential of water hyacinth fibre reinforcement in polymer composites.

Keywords: Natural fibre, Water hyacinth, Polymer composites, Polyethylene, Physio-mechanical properties.

INTRODUCTION

Conventional polymer composites reinforced with fibres typically utilize synthetic fibres in conjunction with a polymer matrix, owing to synthetic fibres cost-effectiveness and commendable mechanical properties [1]. Synthetic fibres exhibit exceptional strength, low weight and high resistance to corrosion, making them well-suited for diverse applications in industries like aerospace, automotive and construction [2]. Despite their advantages, synthetic fibres come with critical drawbacks, including high cost, elevated density compared to polymers and challenges related to recycling and biodegradability.

In contrast, natural fibres offer an environmentally friendly alternative, low density, high specific strength and stiffness contributing to reduced material costs and enhanced safety during handling, processing and utilization compared to synthetic fibres [3-5]. For these reasons, in recent years, natural plant fibres have been increasingly gaining attention as viable alternatives to synthetic fibres [2]. Notably, natural fibres have found applications in manufacturing various automotive parts, as evidenced by studies [6].

Recently, composite production from readily available natural fibre has gained popularity due to its economic viability [7]. Plants that are considered to be problematic and invasive such as water hyacinth, have surfaced as new promising natural fibre sources in recent times [8]. Limited research studies have been conducted on such invasive plants. As such, this study focuses on developing natural fibre reinforced composite using water hyacinth fibre. The water hyacinth is one of the world's most prevalent invasive aquatic plants. It is a free-floating vascular plant known to cause major ecological changes in the environments they invade. The water hyacinth has a direct impact on the water quality by lowering phytoplankton productivity and dissolved oxygen concentrations beneath these mats [9].

The main approaches for the control of aquatic weeds have been classical biological control and mechanical approach supplemented with chemical control [10]. However, all these methods have failed to provide long lasting effects due to the rapid multiplication of the weeds and the relatively low efficacy. When control methods are not successful, extraction and disposal methods are used as an alternative. These include

mechanical extraction of the weed from the water body and dumping on reservoir banks or in vacant lands. When the plant materials are dried enough, they are burnt to reduce the volumes [11]. Open burning of waste materials not only creates greenhouse gasses that contribute to climate change but also damage other important flora and fauna in the area. To address this, the focus of this research is to use fibre from the water hyacinth plant to develop value added products, thereby increasing the productive usability of the plant and reducing the haphazard disposal of the plant that causes environmental pollution. Using a widely available fibre material to develop a new natural fibre composite material could also be economically viable and environmentally friendly compared to using synthetic fibres.

Research indicate that water hyacinth has beneficial properties that makes it a good fibre source in many applications [12]. In plant cell walls, cellulose, hemicellulose and lignin are key components influencing fibre properties [13]. Cellulose, a natural polymer and the primary structural element, imparts remarkable strength and stiffness to plant fibres [14]. Conversely, hemicellulose has been observed to reduce tensile and flexural strength [15]. Studies have revealed that water hyacinth fibres (WHF) have a higher cellulose content compared to coir and date palm fibres [13,16]. Furthermore, water hyacinth can be an ideal reinforcement material in composite development as the plant is found in abundance in the environment and does not require additional care as an agricultural crop or a dedicated fibre plant.

EXPERIMENTAL

In this study, waste polyethylene (PE) bags were obtained from an industry while fresh water hyacinth plants were collected from a water stream near the Karadiyana compost plant in Boralesgamuwa, Sri Lanka. The collected plants were separated from the stem and the stems were utilized as raw materials.

Fibre extraction: Different fibre extraction methods were tested based on the literature, aiming to identify the most efficient and practical approach for fibre extraction.

I. **Solar drying method:** Solar drying for 15 days and dried water hyacinth stems were crushed [17].

II. **Water retting method:** Separated stems were immersed in enclosed bucket and kept for 4 weeks and then the fibres were extracted manually [17].

III. **Decortication:** A decorticator machine was used to extract fibres. Fresh stems were decorticated and decorticated stems were dried [18].

The decorticating method was identified as the most straightforward and efficient fibre extraction technique. Decorticated fibres were subjected to a drying process in a hot air oven at 105 ºC until a constant weight was obtained

General procedure

Composite preparation: Composites were prepared with varying fibre loading (5%, 7.5%, 10% and 12.5%). The necessary weights of both the fibres and polyethylene were accurately measured using a digital weighing machine. Subsequently, the accurately measured dried fibres were cut into lengths of 1-2 cm and positioned between layers of weighed polyethylene, undergoing pre-pressing *via* a pneumatic laminating machine at 140 ºC for 10 min. Following the pre-pressing, the thin sheets were allowed to cool for 10 min. Finally, the pre-pressed sheets were shredded using a mechanical shredder equipped with 1 mm sieve.

The homogeneous crushed particles were placed in a steel mould. Compression was applied using a hot press with upper and lower plates set at 140 ºC, applying 8 MPa pressure for 10 min. The processing temperature was chosen based on the DSC analysis. After unloading the die, the composite manufacturing process was complete and the assembly cooled for 10 min at room temperature before disassembly.

Differential scanning calorimetry (DSC): DSC analysis was carried out to determine the melting point of waste thermoplastic packaging material using a Q200 differential scanning calorimeter from T.A. Instruments. The analysis involved a heating-cooling-heating thermal cycle with temperatures ranging from 30 to 250 ºC and a heating rate of 10 ºC min^{-1}.

Thermogravimetric analysis (TGA): TGA was employed to assess the thermal stability and degradation characteristics of polyethylene (PE) and water hyacinth fibres (WHF) reinforced PE composites. The samples were carefully positioned in platinum pans and subjected to analysis using a TGA machine within a nitrogen atmosphere, maintaining a flow rate of 20 mL min^{-1} to prevent undesired oxidation. The TGA process involved heating both WHF and PE from 30 ºC to 700 ºC at a rate of 10 ºC min^{-1}.

Fourier transform infrared spectroscopy (FTIR): The waste packaging material, WHF underwent FTIR analysis, which was conducted on a Bruker Vertex 80 FTIR spectrophotometer. The ATR mode was utilized for sample analysis, covering a spectral range from 4000 cm^{-1} to 400 cm^{-1} with 128 scans.

Scanning electron microscopy (SEM): The SEM analysis was employed to analyze the tensile fracture surface of the composites. The specimens were scanned using a Hitachi SU6600 scanning electron microscope. The SEM was utilized to investigate the fibre-matrix interaction and failure modes of the tensile specimen.

Tensile test: The test specimens were shaped as per ASTM D 638: Standard test method for tensile properties of plastics. Tensile strength and Young's modulus were determined by using a Testometric M500-50CT tensile testing machine with a standard load cell of 5 KN with a gauge length of 50 mm. Five specimens were tested from each prepared composite and the arithmetic average was calculated.

Flexural test: According to ASTM D 790, the flexural test was carried out in the three-point method to estimate the flexural strength and flexural modulus [19]. Testomeric M500-50CT testing device was used to determine the flexural strength. The ratio of sample thickness to span length was modified to 16:1, as specified in the standard. The crosshead motion rate of the testing device was determined according to eqn. 1. Five specimens were tested from each prepared composite and the arithmetic average was calculated.

$$R = \frac{ZL^2}{6d} \quad (1)$$

Izod impact test: The Izod impact test was conducted following ASTM D 256 standard [20]. V-notched specimens, measuring 63.5 mm × 12.7 mm, were prepared in accordance with the specified standards. Five specimens per composite were tested and the data obtained were used to calculate the average.

Density: The density of the composite materials was evaluated under ASTM D 792 [21]. The procedure involves first measuring the specimen's weight in the air and then determining its weight when fully immersed in distilled water at 23 ºC, utilizing a sinker and wire to ensure complete submersion. The calculations for both density and specific gravity are performed as follows:

$$\text{Specific gravity} = \frac{a}{a + w - b} \quad (2)$$

$$\text{Density } (\rho) = \text{Specific gravity} \times 0.9975 \quad (3)$$

where a is the apparent mass of the specimen, without wire or sinker, in air; b is the apparent mass of specimen (and of sinker, if used) completely immersed and of the wire partially immersed in liquid and w is the apparent mass of totally immersed sinker (if used) and of partially immersed wire.

Hardness: The hardness of the developed thermoplastic composite was assessed using the Shore durometer (MonTech HT 3000), following ASTM D 2240 [22]. To ensure accuracy, an average value was calculated based on ten measurements from each sample.

Flammability test: The flammability of the composites was assessed using the UL-94 Horizontal Flame Propagation test [23]. Three standard samples per composite were tested for flammability, measuring 120 mm × 10 mm × 3.2 mm and were marked with two lines at distances of 25 mm and 100 mm from one end. Each sample was horizontally positioned in the flammability chamber and a controlled bunsen burner flame, applied at a 45º angle, was used to initiate ignition, sustained for 30 s. If the specimen continued burning after 30 s, the time taken for the flame front to travel between the marked lines was measured and the burning rate was expressed in mm min^{-1}.

Water absorption test: According to ASTM D 570, the water absorption properties of the produced composites were assessed [21]. Prior to experimentation, specimens underwent a preconditioning process in a 60 ºC oven for 24 h to eliminate residual moisture and their initial weights were measured precisely. After the initial weighing, composite specimens were immersed in water. At 24 h intervals, the samples were removed, wiped and reweighed to determine water absorption. This process was repeated until reaching a saturation level and the water absorption percentage was calculated using the following equation:

$$WA\ (\%) = \frac{W_n - W_d}{W_d} \times 100 \quad (4)$$

where WA is the water absorption (% w/w); W_n is the weight of wet specimen after soaking and W_d is the initial weight of specimen prior to soaking.

RESULTS AND DISCUSSION

In the initial phase, the most efficient and effective method for extracting fibres was examined. The sunlight drying method did not effectively remove hemicellulose, pectin and waxes. As a result, water retting and mechanical decortication emerged as suitable extraction methods. Upon comparing them, it was observed that mechanical decortication exhibited a higher efficiency in fibre extraction. Consequently, mechanical decortication was chosen as the preferred fibre extraction method.

The waste packaging material was characterized using FTIR-ATR spectrum analysis. The resulting FTIR-ATR spectrum of the waste packaging material exhibited features typical of PE material [24]. It is significant that PE encompasses three distinct types *viz.* low-density polyethylene (LDPE), linear low-density polyethylene (LLDPE) and high-density polyethylene (HDPE), each distinguished by unique crystalline structures. These structural variations can be identified through the analysis of peak intensities in the spectrum. The FTIR-ATR spectrum obtained is presented in Fig. 1. The FTIR analysis of the collected plastic indicated the presence of polyethylene through the identification of doublets at 2914 cm^{-1} and 2848 cm^{-1} that correspond to CH_2 asymmetric stretching. Additionally, deformation doublets were observed at 1470 cm^{-1} and 1465 cm^{-1} due to bending as well as at 718 cm^{-1} due to rocking.

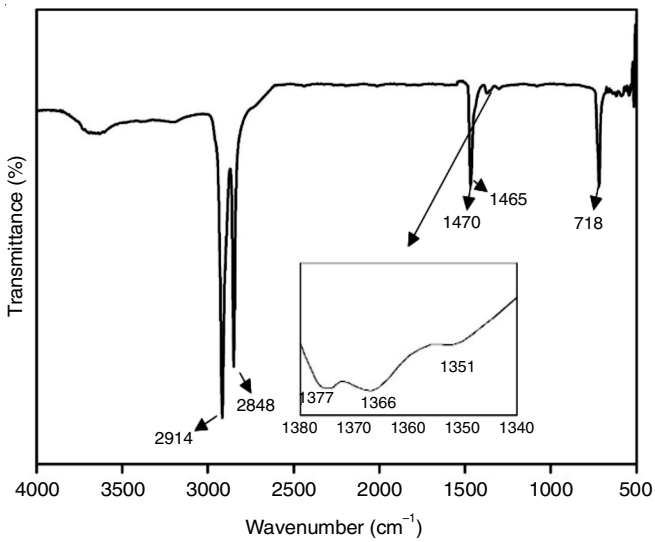

Fig. 1. FTIR spectra of collected plastic material

In Fig. 1, the region between 1340-1380 cm^{-1} is magnified within the same FTIR-ATR spectrum. A notable difference in absorption patterns is evident, revealing three major bands *i.e.* band I at approximately 1377 cm^{-1}, band II at 1366 cm^{-1} and band III at 1351 cm^{-1}, with assignments to CH_2 and CH_3 groups. The differentiation between polyethylene types can be established by the relative strengths of these bands. In LLDPE, band I is weaker than band II. Conversely, in LDPE, band II is stronger than band I. Notably, in HDPE, band I is entirely absent. The peak at 1351 cm^{-1} is a common characteristic among all three types of PE. According to the obtained FTIR-ATR spectrum of waste packaging material, the appearance of peaks at wavenumbers of 1377 cm^{-1} and 1366 cm^{-1} with nearly equal intensity

confirmed that the material is a blend of LDPE and LLDPE [25].

The FTIR-ATR spectrum of the WHF 4000-700 cm^{-1} region is shown in Fig. 2. The absorption peaks observed at 3336 cm^{-1} for WHF correspond to the hydroxyl group (–OH) [26]. The WHF exhibits a CH stretching peak at approximately 2914 cm^{-1}. It has been reported that lignin demonstrates a strong peak at 2920 cm^{-1}, indicating the involvement of lignin aromatic hydrocarbon, methoxyl and methylene groups [26,27]. The absorption band observed at 1728 cm^{-1} in WHF is attributed to the presence of a carbonyl group (C=O) in the acetyl group of hemicellulose. The board absorption band at 1604 cm^{-1} presented to stretching of the benzene ring and $–OCH_3$ groups in the lignin [28]. 1419 cm^{-1} were defined as the C–H bending of amorphous and crystalline cellulose [26,29].

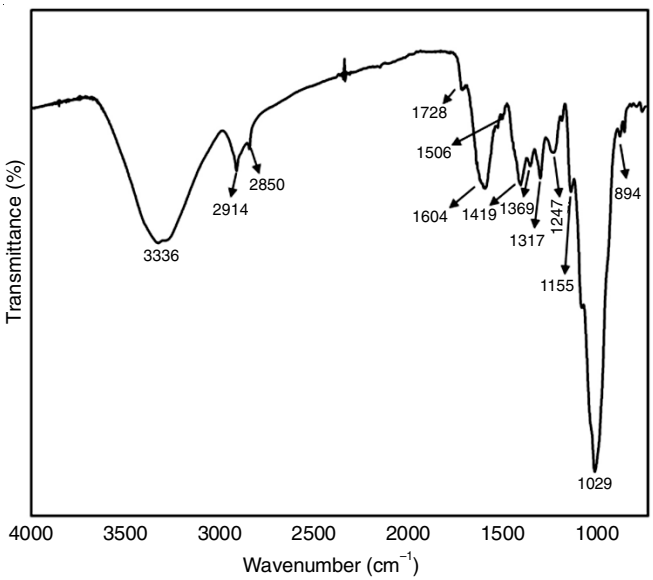

Fig. 2. FTIR spectra of raw WHF

The peak at 1369 cm^{-1} was due to the C-OH stretching of the hydrogen bond intensity of crystalline cellulose. Kabir have reported that an absorption peak around 1373 cm^{-1} was obtained due to the C-OH stretching [26]. The absorption peak at 1317 cm^{-1} corresponds to OH in-plane bending of cellulose. In addition, the absorption band at 1247 cm^{-1} in WHF is assigned to the C=O stretching of (hemicellulose) [27,28]. The band at 1155 cm^{-1} assigned to C–O–C asymmetrical stretching (cellulose and hemicellulose) [28]. Absorbance values at 1029 cm^{-1} represent the presence of C-O [26,30] and O-H stretching vibration, which belongs to polysaccharide in cellulose [27,28,31]. Glycosidic bonds from polysaccharides showed at 894 cm^{-1} [28].

The thermal behaviour of the collected plastic waste was investigated using DSC and TGA as in Fig. 3. The melting points of LDPE and LLDPE were observed at 110 ºC and 118 ºC, respectively. The processing temperature was selected to exceed the melting temperature of the matrix material, as indicated by the DSC analysis [32,33]. The cooling curve of the plastic waste showed exothermic peaks at 99 ºC and 107 ºC, corresponding to the crystallization of LDPE and LLDPE, respectively [25,33].

The TGA curve of the waste packaging material indicates a singular degradation step, commencing at approximately 397.92 ºC and extending until about 509.27 ºC. As reported in the literature, LLDPE begins thermal degradation around 400 ºC, while LDPE degrades within the temperature range of 450-500 ºC [34,35]. Both LLDPE and LDPE exhibit a similar single step degradation process. This alignment between experimental findings and established literature further supports the characterization of the waste packaging material as containing LLDPE/LDPE blend.

The thermal stability of the thermoplastic composites reinforced with WHF, formulated with different weight fractions of the reinforcing material, was evaluated and depicted in Fig. 4. The TGA curve of the matrix without reinforcement exhibited a single degradation step, which corresponded to the primary degradation process of the material. In contrast, the WHF reinforced polymer composites displayed thermal stability up to approximately 50 ºC. The unreinforced matrix did not exhibit such thermal degradation around this temperature. Notably, the slight deviations in the thermograms between 50 ºC and 220 ºC of the WHF reinforced composites indicated the removal of physically absorbed water from the samples. The TGA

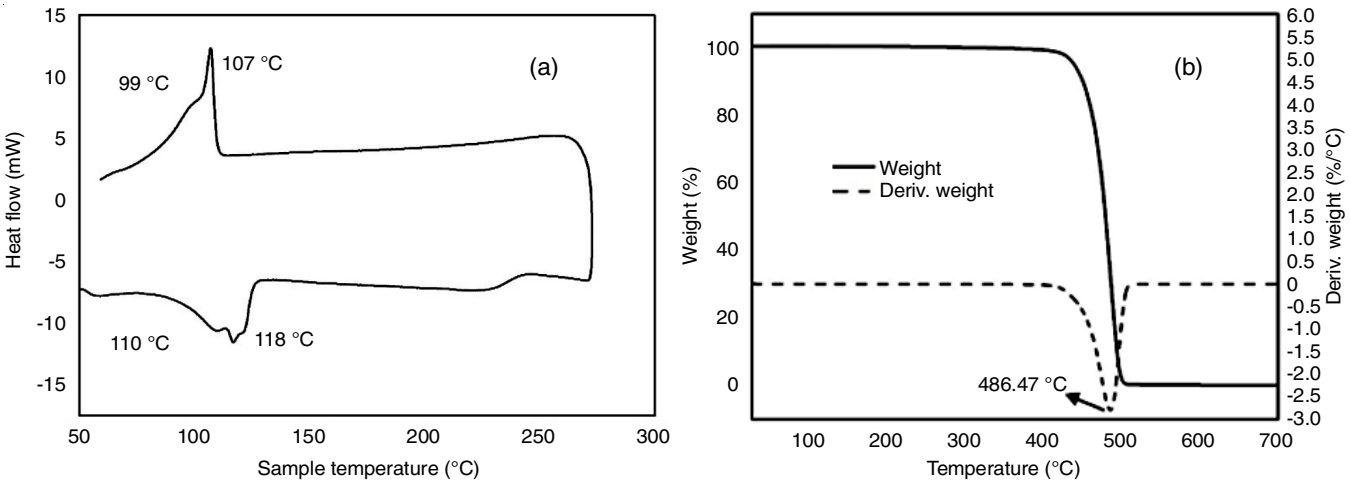

Fig. 3. (a) DSC spectra and (b) TGA and DTG curves of waste packaging material

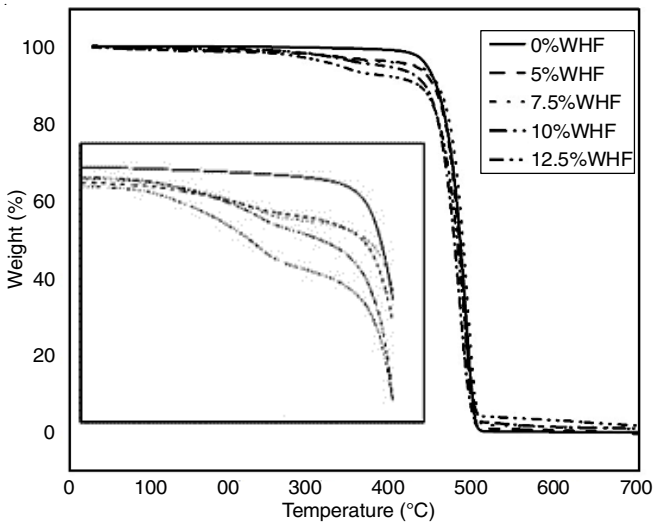

Fig. 4. TGA curves of WHF-reinforced thermoplastic composites (0, 5, 7.5, 10, 12.5 wt% of WHF)

analysis revealed two degradation steps in the fibre reinforced composites. The initial step (270-350 ºC) decomposed hemicellulose and cellulose. The second step, linked to PE matrix decomposition, began around 370 ºC, reaching a maximum temperature of about 480 ºC.

The tensile strength and Young's Modulus values for each prepared composite are illustrated in Fig. 5, along with corresponding standard deviations. The tensile strength of WHF reinforced composites was found to decrease with increasing fibre content. Among the tested compositions, the composites containing 5% and 7.5% WHF demonstrated the highest tensile strengths, measuring 8.6 MPa and 8.3 MPa, respectively. The increase in fibre content resulted in an enlarged weak interfacial area between the PE matrix and WHF. This weak interfacial area can be attributed to the hydrophilic nature of water hyacinth and the hydrophobic nature of the PE matrix as documented in previous studies [36,37]. Additionally, the incorporation of rigid water hyacinth particles into the soft PE matrix may contribute to composite brittleness. As a material becomes more

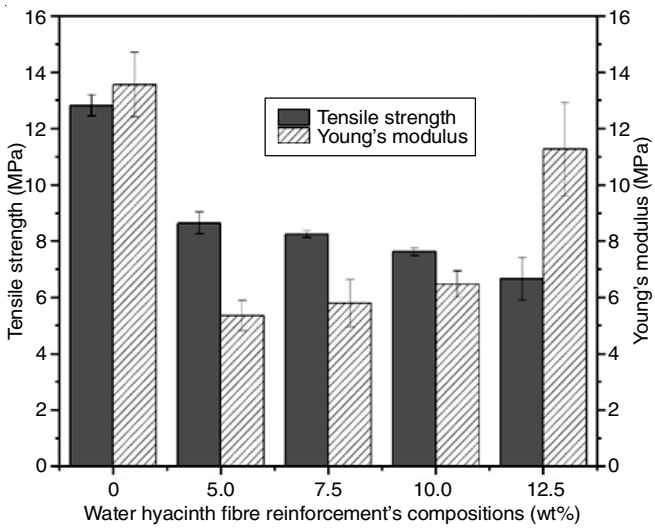

Fig. 5. Tensil strength and Young's modulus of WHF reinforced thermoplastic with different weight percentages of WHF

brittle, its strength decreases while its stiffness increases. Furthermore, the Young's modulus of WHF-reinforced composites displayed an increasing trend. The findings indicate that the addition of rigid fibres to the soft thermoplastic PE matrix enhances the rigidity of the composite.

Fractographic analysis was conducted to investigate the failure mechanisms exhibited during tensile testing of specimens reinforced with 7.5 wt. % WHF. The SEM micrographs were obtained to examine the fractured surfaces of the specimens. Analysis of the tensile-fractured surfaces utilizing the electron microscope (Fig. 6) revealed that the thermoplastic composite experienced failure during the tensile test primarily due to common failure mechanisms, including poor interfacial interaction and fibre-matrix de-bonding. The microstructure of composite exhibited numerous cavities and pulled-out fibres, indicating weak bonding between the fibres and the polymer matrix. Consequently, the fracture surface of the composite predominantly exhibited the presence of pulled-out fibres rather than fibre breakage. Furthermore, the examination revealed localized clusters of WHF and patches of PE matrix, which indicated insufficient dispersion of the fibre material within the PE matrix. Additionally, minor cracks were observed within the composite.

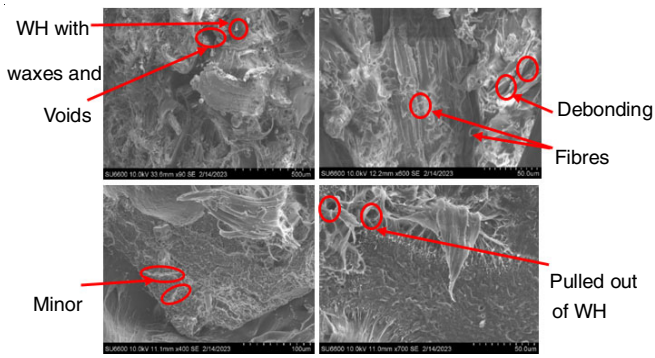

Fig. 6. SEM images of the tensile fractured surface of 7.5% WHF reinforced tensile fractured surfaces

The flexural strength and flexural modulus values for each prepared composite are illustrated in Fig. 7, along with corresponding standard deviations. It was observed that the flexural strength and flexural modulus exhibited a gradual increase with increasing fibre loading. Notably, the composite containing 12.5% WHF displayed the highest flexural strength and flexural modulus, with values of 10.1 MPa and 210.5 MPa, respectively. This improvement in flexural properties can be attributed to the effective reinforcement and stress transmission from the thermoplastic matrix to the incorporated WHF. Furthermore, the increase in flexural strength can be ascribed to the improved interaction between the fibres and matrix, particularly under compressive stresses experienced during bending. This enhanced interaction occurs within the transverse section of the flexural specimens, regardless of the surface condition of the fibres, as supported by previous research [38]. These findings suggest that an appropriate amount of fibre loading can enhance the flexural properties of thermoplastic composites reinforced with WHF.

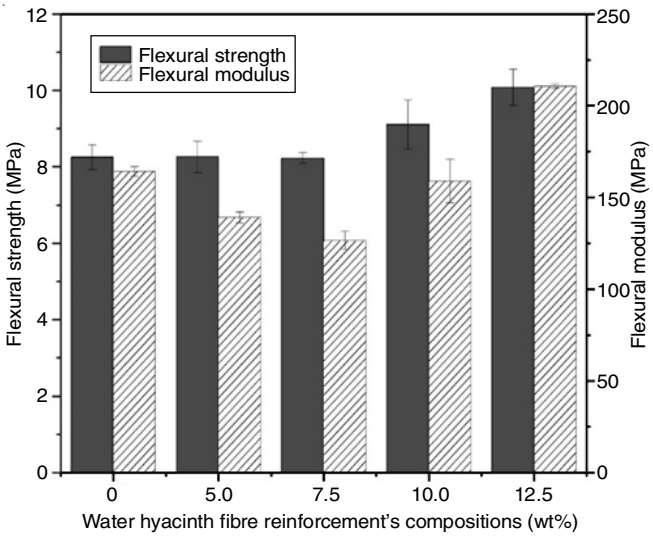

Fig. 7. Flexural strength and flexural modulus of WHF reinforced thermoplastic with a different weight percentage of WHF

The Izod impact results of each weight percentage of WHF reinforced composites are shown in Fig. 8. The capacity of a material to withstand the application of high-speed fracture under stress is known as impact strength. The total toughness of composite material is strongly correlated with their impact characteristics [39,40]. The Izod impact strengths of WHF reinforced composites were increased with increasing WHF wt.%. Significantly, the composite with 12.5% WHF demonstrated the highest impact strength at 26 J m^{-1} compared to other WHF-reinforced composites. The impact strength of the 12.5% WHF-reinforced composite surpassed that of the control sample. These results indicate that an increase in WHF loading contributes positively to energy absorption. The density measurements of the prepared composites are presented in Fig. 9.

The control sample, which contained 0% WHF, exhibited a density of 0.93 g cm^{-3}. As the WHF content increased, the density values of the composites decreased. Specifically, the density of the thermoplastic composite reinforced with WHF ranged between 0.89 and 0.93 g cm^{-3}. This observation may be attributed to the low density of WHF or voids in the prepared composites, as discussed in the fractographic analysis. In comparison, a previous study reported the density of WHF as 0.226 g cm^{-3} [16]. The density of this particular fibre is remarkably low when compared to that of other synthetic fibres. Based on this value and the obtained results, it can be concluded that polymer composites reinforced with WHF are suitable for lightweight applications.

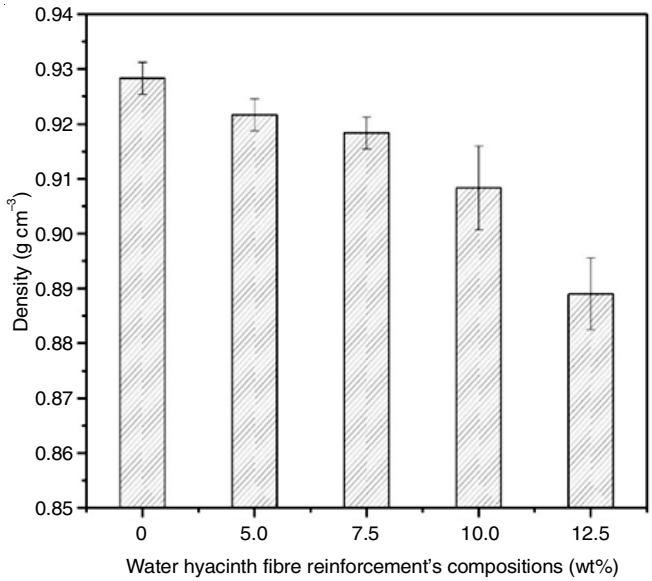

Fig. 9. Density of WHF-reinforced thermoplastic composite with different weight percentages of WHF

The shore D hardness values for each prepared composite are illustrated in Fig. 10, along with corresponding standard deviations. The resistance of the composites to permanent indentation was evaluated using the hardness (shore D) test [41]. According to the results, the hardness of composites has increased gradually with increasing fibre loading.

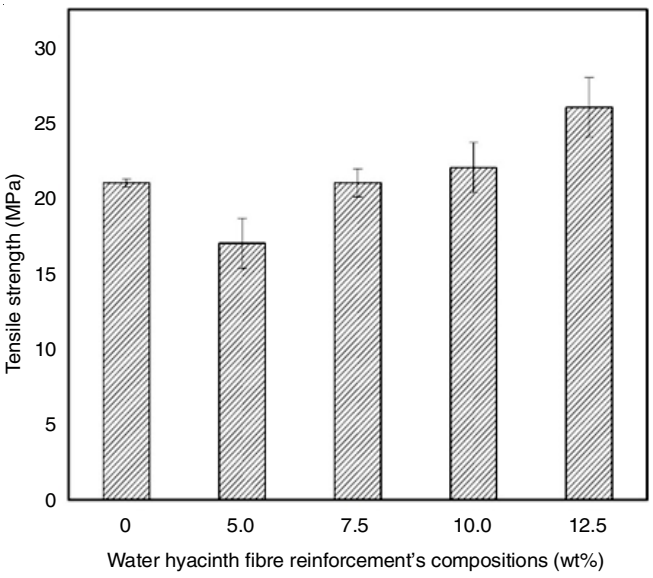

Fig. 8. Izod impact strength of WHF reinforced thermoplastic composite with different weight percentages of WHF

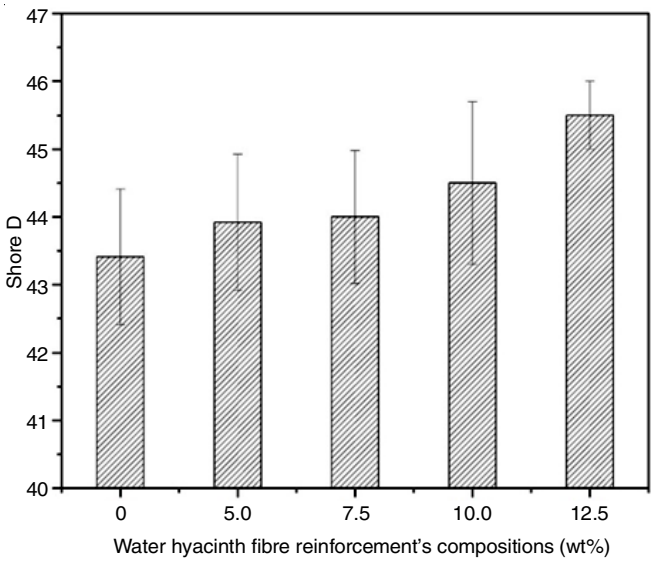

Fig. 10. Shore D hardness of Water hyacinth fibre-reinforced thermoplastic composite with different weight percentages of Water hyacinth fibres

When selecting a material for a specific application, it is important to consider its susceptibility to water absorption, as it can potentially lead to a decline in certain desirable properties [37]. To assess this, the weight growth percentages and water absorption were calculated at regular intervals. Fig. 11 presents a comparison of the changes in weight increase percentages over time for thermoplastic composite specimens reinforced with water-immersed WHF, incorporating various WHF loadings.

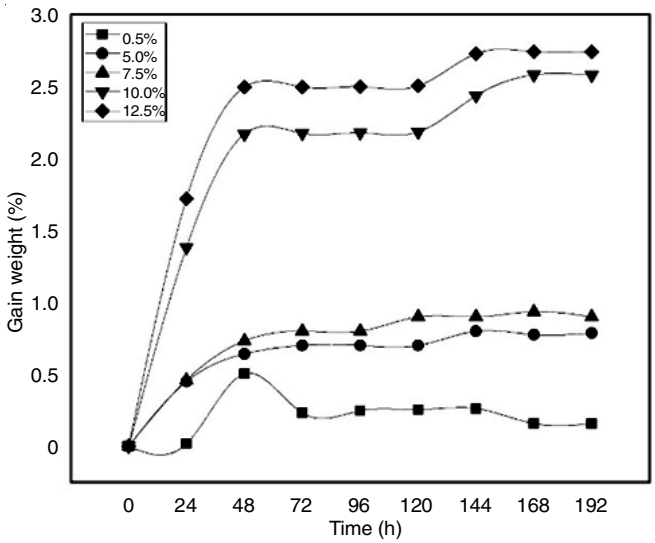

Fig. 11. Moisture absorption percentage of WHF-reinforced thermoplastic composite with different weight percentages of WHF *vs*. time (h)

Upon reaching an equilibrium state, the rate of water absorption in the tested samples exhibited gradual reduction, following an initial period of accelerated absorption within the first few days (0-48 h). Notably, the equilibrium state is observed to be achieved after 144 h. The results indicate a positive correlation between the weight percentage of WHF and the extent of moisture absorbance, with higher WHF weight percentages leading to increased water absorption. Among the WHF-reinforced composites, the thermoplastic composite with a 12.5% WHF loading demonstrated the highest water absorption percentage, reaching 2.74%.

Natural fibre-reinforced polymer composites have the ability to absorb moisture/water from the surrounding atmosphere due to the presence of hydroxyl groups within the natural fibres, as suggested in prior studies [42,43]. In this study, the experimental results have shown that the hydroxyl group content of WHF reinforced thermoplastic composite increased with increasing WHF content, leading to an increase in water absorbance. This phenomenon is further influenced by the increase in micro voids with increasing fibre load [37]. Examination of the SEM micrographs obtained to examine the fractured surfaces of the specimens can provide further insight into the impact of micro voids on moisture absorption.

The summarized findings of the flammability tests are presented in Table-1. The results indicate that the burning rate of composites reinforced with WHF exhibited an increase as the weight percentage of WHF increased. The reason for increasing flammability is the combustible nature of cellulosic fibrous materials [44].

TABLE-1
RESULTS OF FLAMMABILITY TESTS PERFORMED ON PE THERMOPLASTIC COMPOSITES USING VARIOUS WEIGHT COMPOSITIONS OF WHF REINFORCEMENT

Sample name with WHF weight percentage	Burning rate (mm min^{-1})
0.0% WHF	28.7
5.0% WHF	30.9
7.5% WHF	31.5
10.0% WHF	31.4
12.5% WHF	31.6

Comparative analysis of physico-mechanical properties of novel composite materials with commercial alternatives: The results of the current research study were compared with those of commercially available products and findings from related research articles, as summarized in Table-2. The tensile strength of WHF reinforced PE composites was determined to be higher than that of the referenced commercially available products and other sources in the comparison [45]. The flexural strength results from the current study fall within an acceptable range when compared with other sources [45-48]. Additionally, the water absorption value of the WHF reinforced PE composite was found to be lower than that of the referenced commercially available products and other sources in the comparison.

Conclusion

Based on the results of thermal and FTIR analyses, the plastic material composition was identified as a blend of LDPE and LLDPE. The experimental data revealed a decreasing trend

TABLE-2
PHYSICAL PROPERTIES AND MECHANICAL PROPERTIES OF OTHER TYPES OF PRODUCTS

Properties	Water hyacinth fibre reinforced PE composite	Commercial wood particleboard-general purpose	Trilite ceiling	Medium-Density Fibreboard from giant bamboo	Palm rachis particleboard (1-0.25 mm)	Asbestos ceiling board
Tensile strength (MPa)	8.4-6.7	6	NA	0.10-0.26	NA	NA
Young's modulus (MPa)	5.6-10.1	1800	5000-6000	NA	NA	NA
Flexural strength (MPa)	8.3-10.35	11.5	12.1-17.1	9.28-11.10	13.97	1.0-3.0
Flexural modulus (MPa)	139-210.5	550	NA	877.45-1297.51	1567.16	NA
Shore hardness (HD)	44-47	NA	NA	NA	NA	NA
Density (g cm^{-3})	0.89-0.92	0.5-0.8	1-1.05	0.84-0.76	0.856	1.5-1.95
Water absorption (%)	0.78-2.74	70	35	14.91-28	85.91	0.5-3
Ref.	Present study	[45]	[47]	[46]	[45]	[46]

in tensile strength with increasing WHF content. However, the flexural and Izod impact strengths showed positive improvements when WHF was used as a reinforcement in thermoplastic composites. The density of WHF-reinforced polymer composites decreased with increasing WHF content. The water absorption of the composite increased with the inclusion of WHF, attributed to the increased presence of hydroxyl groups and micro voids. Additionally, the burning rate of the composites increased with increasing WHF content. Overall, the 5%, 7.5% and 10% WHF-reinforced composites exhibited optimum mechanical properties compared to other compositions. The results of this study highlight that the developed composite possesses properties comparable to those of commercial particleboards and aligns with reported findings. This study underscores the promising potential of utilizing WHF to create value-added high-quality composite materials. The use of an invasive aquatic weed for value-added applications not only contributes to managing the disposal of the aquatic weed using unsustainable methods such as open burning but also provides a valuable natural fibre source for material development.

ACKNOWLEDGEMENTS

Financial assistance by University of Sri Jayewardenepura research grant: ASP/01/RE/TEC/2021/80.

CONFLICT OF INTEREST

The authors declare that there is no conflict of interests regarding the publication of this article.

REFERENCES

1. H. Ku, H. Wang, N. Pattarachaiyakoop and M. Trada, *Compos., Part B Eng.*, **42**, 856 (2011); https://doi.org/10.1016/j.compositesb.2011.01.010
2. I. Elfaleh, F. Abbassi, M. Habibi, F. Ahmad, M. Guedri, M. Nasri and C. Garnier, *Results Eng.*, **19**, 101271 (2023); https://doi.org/10.1016/j.rineng.2023.101271
3. H. Danso, *Procedia Eng.*, **200**, 1 (2017); https://doi.org/10.1016/j.proeng.2017.07.002
4. N. Flores-Ramirez, Y. Sanchez-Hernandez, J. Cruz de Leon, S.R. Vasquez-Garcia, L. Domratcheva-Lvova and L. Garcia-Gonzalez, *Fibers Polym.*, **16**, 196 (2015); https://doi.org/10.1007/s12221-015-0196-5
5. K.L. Pickering, M.G.A. Efendy and T.M. Le, *Compos., Part A Appl. Sci. Manuf.*, **83**, 98 (2016); https://doi.org/10.1016/j.compositesa.2015.08.038
6. S.A. Tewelde, H.G. Lemu and J.B. Dawit, *Mater. Today Proc.*, **62**, 6445 (2022); https://doi.org/10.1016/j.matpr.2022.04.115
7. R. Sindhu, P. Binod, A. Pandey, A. Madhavan, J.A. Alphonsa, N. Vivek, E. Gnansounou, E. Castro and V. Faraco, *Bioresour. Technol.*, **230**, 152 (2017); https://doi.org/10.1016/j.biortech.2017.01.035
8. S. Bordoloi, V. Kashyap, A. Garg, S. Sreedeep, L. Wei and S. Andriyas, *Measurement*, **113**, 62 (2018); https://doi.org/10.1016/j.measurement.2017.08.044
9. A. Malik, *Environ. Int.*, **33**, 122 (2007); https://doi.org/10.1016/j.envint.2006.08.004
10. M. Schwarzländer, H.L. Hinz, R.L. Winston and M.D. Day, *BioControl*, **63**, 319 (2018); https://doi.org/10.1007/s10526-018-9890-8
11. D.M.N.S. Dissanayaka, S.S. Udumann, D.K.R.P.L. Dissanayake, T.D. Nuwarapaksha and A.J. Atapattu, *Waste*, **1**, 264 (2023); https://doi.org/10.3390/waste1010017
12. V. Guna, M. Ilangovan, M.G. Anantha Prasad and N. Reddy, *ACS Sustain. Chem. Eng.*, **5**, 4478 (2017); https://doi.org/10.1021/acssuschemeng.7b00051
13. F.M. Al-Oqla and S.M. Sapuan, *J. Clean. Prod.*, **66**, 347 (2014); https://doi.org/10.1016/j.jclepro.2013.10.050
14. D. Kumaravel, P. Gopal and V.K. Bupesh Raja, *Appl. Mech. Mater.*, **766–767**, 57 (2015); https://doi.org/10.4028/www.scientific.net/AMM.766-767.57
15. M.Y. Khalid, A. Al Rashid, Z.U. Arif, W. Ahmed, H. Arshad and A.A. Zaidi, *Results Eng.*, **11**, 100263 (2021); https://doi.org/10.1016/j.rineng.2021.100263
16. A. Arivendan, W.J. Jebas Thangiah, S. Irulappasamy and B.N. Chrish, *J. Ind. Text.*, **51(5_suppl)**, 8157S (2022); https://doi.org/10.1177/15280837211067281
17. A. Ajithram, J.T.W. Jappes and N.C. Brintha, *Mater. Today: Proc.*, **45**, 1626 (2021); https://doi.org/10.1016/j.matpr.2020.08.472
18. S. George, S. Thomas, N. Nandanan Nedumpillil and S. Jose, *J. Nat. Fibers*, **20**, 2212927 (2023); https://doi.org/10.1080/15440478.2023.2212927
19. T. Thamae, R. Marien, L. Chong, C. Wu and C. Baillie, *J. Mater. Sci.*, **43**, 4057 (2008); https://doi.org/10.1007/s10853-008-2495-3
20. J.R. Wagner, E.M. Mount and H.F. Giles, 'Testing Properties', in *Extrusion*, Elsevier, 241 (2014); https://doi.org/10.1016/B978-1-4377-3481-2.00021-1
21. N. Saba, M. Jawaid and M.T.H. Sultan, An Overview of Mechanical and Physical Testing of Composite Materials, In: Mechanical and Physical Testing of Biocomposites, Fibre-Reinforced Composites and Hybrid Composites, Woodhead Publishing Series in Composites Science and Engineering (2019); https://doi.org/10.1016/B978-0-08-102292-4.00001-1
22. G. Pinto and M.B. Maidana, *J. Appl. Polym. Sci.*, **82**, 1449 (2001); https://doi.org/10.1002/app.1983
23. C.A. Echeverria, W. Handoko, F. Pahlevani and V. Sahajwalla, *J. Clean. Prod.*, **208**, 1524 (2019); https://doi.org/10.1016/j.jclepro.2018.10.227
24. J.V. Gulmine, P.R. Janissek, H.M. Heise and L. Akcelrud, *Polymer Testing*, **21**, 557 (2002); https://doi.org/10.1016/S0142-9418(01)00124-6
25. J. Korol, A. Hejna, K. Wypiór, K. Mijalski and E. Chmielnicka, *Polymers*, **13**, 1383 (2021); https://doi.org/10.3390/polym13091383
26. M.M. Kabir, H. Wang, K.T. Lau and F. Cardona, *Appl. Surf. Sci.*, **276**, 13 (2013); https://doi.org/10.1016/j.apsusc.2013.02.086
27. S.J. Tan and A.G. Supri, *Polym. Bull.*, **73**, 539 (2016); https://doi.org/10.1007/s00289-015-1508-z
28. N. Sumrith, L. Techawinyutham, M.R. Sanjay, R. Dangtungee and S. Siengchin, *J. Polym. Environ.*, **28**, 2749 (2020); https://doi.org/10.1007/s10924-020-01810-y
29. M. Maslowski, J. Miedzianowska and K. Strzelec, *J. Polym. Environ.*, **26**, 4141 (2018); https://doi.org/10.1007/s10924-018-1285-5
30. M.M. Netai, K. Jameson and F.Z. Mark, *Afr. J. Biotechnol.*, **15**, 897 (2016); https://doi.org/10.5897/AJB2015.15068
31. G. Rajeshkumar, V. Hariharan and T. Scalici, *J. Nat. Fibers*, **13**, 702 (2016); https://doi.org/10.1080/15440478.2015.1130005
32. J. Cran, Ph.D. Thesis, Characterization and Optimization of Polyethylene Blends, Victoria University of Technology, Melbourne, Australia (2004).
33. D. Li, L. Zhou, X. Wang, L. He and X. Yang, *Materials*, **12**, 1746 (2019); https://doi.org/10.3390/ma12111746
34. M. Bhatia, A. Girdhar, A. Tiwari and A. Nayarisseri, *Springerplus*, **3**, 497 (2014); https://doi.org/10.1186/2193-1801-3-497
35. D.G. Dikobe and A.S. Luyt, *Express Polym. Lett.*, **4**, 729 (2010); https://doi.org/10.3144/expresspolymlett.2010.88
36. A.G. Supri, S.J. Tan, H. Ismail and P.L. Teh, *Polym. Plast. Technol. Eng.*, **50**, 898 (2011); https://doi.org/10.1080/03602559.2011.551981

37. M. Saha and A.M. Afsar, *Int. J. Eng. Mater. Manufacture*, **3**, 151 (2018); https://doi.org/10.26776/ijemm.03.03.2018.04
38. F.Z. Arrakhiz, M. El Achaby, M. Malha, M.O. Bensalah, O. Fassi-Fehri, R. Bouhfid, K. Benmoussa and A. Qaiss, *Mater. Des.*, **43**, 200 (2013); https://doi.org/10.1016/j.matdes.2012.06.056
39. S. Mishra, A.K. Mohanty, L.T. Drzal, M. Misra, S. Parija, S.K. Nayak and S.S. Tripathy, *Compos. Sci. Technol.*, **63**, 1377 (2003); https://doi.org/10.1016/S0266-3538(03)00084-8
40. S. Öztürk, *J. Compos. Mater.*, **44**, 2265 (2010); https://doi.org/10.1177/0021998310364265
41. M. Andó, G. Kalácska and T. Czigány, *Sci. Bull., Series C: Fascicle Mechanics, Tribol., Machine Manufact. Technol.*, **23**, 15 (2009).
42. J.A. Halip, L.S. Hua, Z. Ashaari, P.M. Tahir, L.W. Chen and M.K. Anwar Uyup, Effect of Treatment on Water Absorption Behavior of Natural Fiber-Reinforced Polymer Composites, In: Mechanical and Physical Testing of Biocomposites, Fibre-Reinforced Composites and Hybrid Composites, Woodhead Publishing Series in Composites Science and Engineering, Chap. 8, pp. 141-156 (2019); https://doi.org/10.1016/B978-0-08-102292-4.00008-4
43. E. Muñoz and J.A. García-Manrique, *Int. J. Polym. Sci.*, **2015**, 1 (2015); https://doi.org/10.1155/2015/390275
44. N.K. Kim, S. Dutta and D. Bhattacharyya, *Compos. Sci. Technol.*, **162**, 64 (2018); https://doi.org/10.1016/j.compscitech.2018.04.016
45. T. Hamouda, A.H. Hassanin, N. Saba, M. Demirelli, A. Kilic, Z. Candan and M. Jawaid, *J. Polym. Environ.*, **27**, 489 (2019); https://doi.org/10.1007/s10924-019-01369-3
46. N.P. Marinho, E.M. Nascimento, S. Nisgoski and I.D. Valarelli, *Mater. Res.*, **16**, 1387 (2013); https://doi.org/10.1590/S1516-14392013005000127
47. P.S.E. Ang, A.H.I. Ibrahim and M.S. Abdullah, *Progr. Eng. Appl. Technol.*, **1**, 104 (2020).
48. C.E. Ferrández-García, A. Ferrández-García, M. Ferrández-Villena, J.F. Hidalgo-Cordero, T. García-Ortuño and M.T. Ferrández-García, *Forests*, **9**, 755 (2018); https://doi.org/10.3390/f9120755